Tabriz Journal of Electrical Engineering (TJEE), vol. 56, no. 1, 2026 Serial no. 115
DOI: 10.22034/tjee.2025.67507.5029

Maximum Power Point Tracking (MPPT) of a Photovoltaic System Connected to a Microgrid under Partial Shading Conditions Using the Gravitational Search Algorithm (GSA)

Asaad Shemshadi[a*], Mehdi Payamani[b]

[a] Department of Power Electrical Engineering,School of electrical engineering, Arak University of Technology, Arak, Iran, Email:shemshadi@arakut.ac.ir
[b] Department of Power Electrical Engineering,School of electrical engineering, Arak University of Technology, Arak, Iran, Email:mhd.payamani@gmail.com

[*]Asaad Shemshadi, Assistant professor of Arak University of Technology, electrical engineering department, Arak, Iran.

Received:: 26/05/2025, Revised: 19/09/2025, Accepted: 05/11/2025.

Abstract

Photovoltaic (PV) systems are increasingly integrated into microgrids, offering clean and sustainable energy solutions. However, partial shading conditions significantly impact PV system performance, leading to multiple local maxima in the power-voltage (P-V) curve. This necessitates robust Maximum Power Point Tracking (MPPT) algorithms to extract maximum power efficiently. This paper proposes a novel MPPT technique for PV systems connected to a microgrid under partial shading conditions, employing the Gravitational Search Algorithm (GSA). GSA, inspired by Newtonian gravity, effectively explores the solution space and converges towards the global maximum power point. The proposed method is evaluated through simulations, demonstrating superior performance compared to conventional MPPT techniques in terms of tracking accuracy, convergence speed, and robustness against varying shading patterns. The graph of the tracked power for the proposed method in this paper, under variable temperature and partial shading conditions, shows that it has a faster response (100ms) compared to similar methods, such as the Fuzzy Logic Controller (FLC) and the Gravitational Search Algorithm (GSA), for tracking the global maximum power point in grid-connected PV systems under partial shading conditions. The results highlight the effectiveness of the GSA-based MPPT in maximizing energy extraction from PV systems under challenging operating conditions, thereby enhancing the overall efficiency and reliability of microgrids.

Keywords
Maximum Power Point Tracking, Gravitational Search Algorithm, Photovoltaic System, Partial Shading Condition.

1. Introduction

The extensive use of fossil fuels such as oil, coal, and gas has led to greenhouse effects and environmental pollution. Meanwhile, there is a significant discrepancy between fossil fuel resources and global energy demand. Energy shortages and environmental pollution have become major obstacles to human development [1]. Solar energy is one of the free, clean, and environmentally friendly energy sources that has been utilized by humans in various ways since ancient times. Although the cost of using solar energy is relatively high, modern energy policies do not solely focus on the expense of solar systems. Instead, the benefits of utilizing these systems, such as reducing environmental pollution, are also taken into account [2]. Photovoltaic (PV) energy has emerged in recent years as a reliable, clean, and unlimited energy source. However, the high initial installation cost and the low energy conversion efficiency are among the primary disadvantages of using photovoltaic systems. Extensive efforts have been made, and continue to be made, to mitigate the aforementioned drawbacks by improving the energy conversion efficiency through enhancing the quality of solar cells and maximizing the power output from solar cells. The characteristics of photovoltaic (PV) systems are inherently nonlinear and are influenced by environmental parameters, such as irradiation, ambient temperature, and the connected load. By appropriately selecting the operating point of the PV array, maximum power can be extracted under constant irradiation and temperature conditions. As environmental conditions (irradiation and temperature) change, the operating point of the array also shifts. Consequently, different Maximum Power Point Tracking (MPPT) algorithms are employed to ensure that the power output of the array remains at its maximum level, effectively tracking the maximum power point. Various methods exist for MPPT, including Hill-Climbing, Perturb and Observe (P&O), Incremental Conductance, Fuzzy Logic Control, Parasitic Capacitance, Ripple-Based Control, and others. In these methods, the solar arrays are typically fixed. However, as the sun moves and the angle of sunlight on the array changes, the power output from the PV array decreases. Nonetheless,

extracting maximum power from the PV array under varying environmental conditions remains crucial. Using an MPPT system ensures that the system is continuously adjusted to provide maximum power, regardless of environmental or load conditions [3, 4]. In [34], a new neuro-fuzzy controller is presented for Maximum Power Point Tracking (MPPT) in grid-connected photovoltaic (PV) systems under partial shading conditions. This method tracks the maximum power point with high speed and accuracy, thereby improving tracking speed and output power compared to traditional methods. However, neuro-fuzzy controllers require specialized expertise to design membership functions and rule tables, and the combination of algorithms can lead to computational complexity. Ref [43] introduces an innovative hybrid MPPT approach called WSO-IC, which combines the War Strategy Optimization (WSO) algorithm with the Incremental Conductance (IC) method for PV systems under constant partial shading. The main achievement of this method is its superior MPPT performance with faster convergence, high efficiency (over 99%), and minimal oscillation around the maximum power point. However, the WSO-IC algorithm has a higher implementation cost compared to conventional MPPT methods. A comprehensive review of MPPT methods in solar PV systems is provided in [44], covering both conventional and AI-based algorithms with a focus on partial shading conditions. Its primary objective is to summarize sequential developments, review trends, and classify different control strategies along with their advantages and disadvantages. Conventional methods like P&O suffer from steady-state oscillations and low tracking speed under partial shading conditions, while AI-based methods can have computational complexity and a dependency on training data. In [45], the Dandelion Optimizer (DO) algorithm is proposed as a meta-heuristic optimization technique to achieve MPPT in PV arrays under partial shading. This algorithm demonstrates better performance in terms of power tracking efficiency, tracking time, and tracked maximum power compared to PSO and CS, achieving an average efficiency of 99.60% in HIL results. Ref [35] investigates an MPPT controller for microgrids using a combination of the Gravitational Search Algorithm (GSA) and the Adaptive Neuro-Fuzzy Inference System (ANFIS). By leveraging the adaptive capabilities of ANFIS and the optimization power of GSA, this method improves the stability, reliability, and PV power conversion efficiency, especially under varying atmospheric conditions. However, the ANFIS-GSA method requires a training phase to tune the neuro- and fuzzy-system parameters, which can involve a large volume of computational data. Ref [36] applies the Hypersphere Search (HSS) algorithm to track the Global Maximum Power Point (GMPP) in solar PV systems under partial shading conditions. This method is simple to implement, shows high exploration and exploitation power, has fast convergence and low steady-state oscillations, and never gets stuck in local maxima. Ref [37] provides a classification and comparison of various MPPT techniques for photovoltaic systems, including offline, online, and hybrid methods. Its main conclusion is that hybrid methods, despite their higher complexity, outperform conventional methods under similar operating conditions, thereby improving the system's efficiency and dynamic response. Offline methods, such as OCV and SCC, have low accuracy and require load disconnection, which leads to power loss, while online methods like P&O suffer from oscillations and complexity. An Adaptive Particle Swarm Optimization (APSO) algorithm is introduced in [38] for MPPT in PV systems under partial shading conditions. By adaptively adjusting its learning factors and inertia weight, APSO improves convergence speed and accuracy and reduces power oscillations during the tracking process. In [39], the Butterfly Optimization Algorithm (BOA) is implemented for MPPT in PV systems to mitigate the effects of Partial Shading Condition (PSC). This method shows high accuracy and better tracking speed to reach the GMPP compared to the PSO-GSA and GWO algorithms, making it a promising alternative for real-time applications. Ref [40] presents a new hybrid approach for MPPT based on a Fuzzy Logic Controller (FLC) and the GSA for tracking the global maximum power point in grid-connected PV systems under partial shading conditions. This method demonstrates fast and accurate performance in tracking the MPP under variable and partial shading conditions. In [41], a modified PSO-based MPPT algorithm with damped inertia weight and time-varying acceleration coefficients (PSODTVAC) is applied to PV systems under partial shading. Compared to GSA, standard PSO, and PSOTVAC, PSODTVAC offers better performance in tracking efficiency and convergence speed, especially under complex and dynamic conditions, which reduces the number of iterations and power losses. Ref [42] investigates the hybrid HPSO-GSA algorithm for MPPT in PV systems under partial shading conditions. By combining the strengths of PSO and GSA, this method offers faster convergence, higher power efficiency, and lower oscillations compared to the individual PSO and GSA algorithms at different irradiance levels. In [46], a new method is presented for determining and tracking the GMP of a solar array by measuring the irradiance and temperature on each solar panel. This smart algorithm is implemented using an STM32 microcontroller. A disadvantage of this method is the need for separate sensors to measure the irradiance and temperature for each panel, which can increase system complexity and cost. Ref [47] describes a new method for tracking the global maximum power point in solar arrays with multiple parallel strings under partial shading conditions. The method first estimates the maximum power point voltage for each parallel string in the array. Then, by applying these voltages to the power converter and comparing the output power, the point that produces the highest power is selected as the array's GMPP. One of the disadvantages of this method is that its accuracy depends on the initial estimation of the GMPP voltage for each string; an inaccurate estimation will increase the final error. In previous studies, the output current of the system is often controlled in current-mode operation. Based on a review of the literature, PV systems are primarily defined as current sources in the grid and are controlled solely for active power generation. This paper proposes a control method for photovoltaic systems and inverters aimed at voltage stabilization. For voltage control, the existing equipment in the PV system is utilized, and with

additional capacity considered for the inverter, both active and reactive power are generated.

2. Maximum Power Point Tracking (MPPT) in Grid-Connected Solar Cells

The model of a solar cell can be represented as the circuit diagram shown below. The current-voltage (I-V) characteristic of a solar cell is illustrated in the accompanying graph. To achieve maximum power output from the solar cell, its operating point must be set at the optimal point. The voltage and current at this optimal operating point are denoted as V_{max} and I_{max}, respectively.

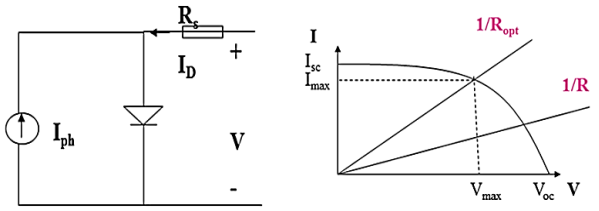

Fig.1. The circuit diagram of a solar cell and the current-voltage (I-V) curve of the solar cell.

To achieve the desired voltage and current, solar cells are connected in series and parallel configurations. The figure below illustrates the current-voltage (I-V) curves for two solar cells in series and parallel arrangements. Connecting the cells in series increases the voltage, while parallel connection enhances the current capacity.

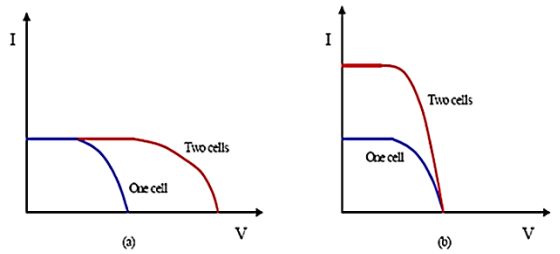

Fig.2. The current-voltage (I-V) curve, series and parallel connection of two solar cells.

With changes in light intensity and ambient temperature, the current-voltage (I-V) curve of each solar cell (Figure 1) and, consequently, the curve for the entire modules and arrays are affected. As a result, the voltage and current characteristics of the optimal operating point also change. To ensure the arrays operate at their optimal point, Maximum Power Point Tracking (MPPT) methods are employed. Various techniques can be used to achieve the maximum power point. The adjustment of the operating voltage and current of the cells is carried out by a DC/DC converter. One simple method for tracking the maximum power point is described here.

Changes in the operating voltage and current of the cells lead to variations in output power. If increasing or decreasing the voltage and current results in higher output power, the adjustment continues in the same direction until a decrease in power is observed. When further changes in voltage and current cause a reduction in output power, the system holds the operating point at that specific value, which corresponds to the optimal point. This method works effectively because there is only one maximum point in the power-voltage (P-V) curve of the array. The system that performs this optimization is referred to as an MPPT system (Figure 3) [14].

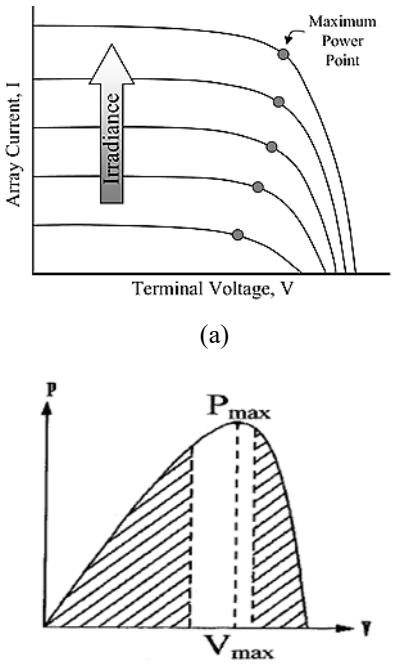

Fig.3. The Effect of Increasing Light Intensity on the Current-Voltage Curve and Power-Voltage Curve.

Figure 3 examines the effect of changes in light intensity on the I-V (current-voltage) and P-V (power-voltage) curves. This figure consists of two main graphs:

Graph (a) (I-V Curves): This graph shows the effect of increasing solar irradiance on the current-voltage curve. As the upward-pointing arrow indicates, the curve shifts upwards with an increase in irradiance. This means that for any given voltage, the array's output current increases. The marked points on each curve represent the maximum power point (MPP) for that specific irradiance level. As irradiance increases, these points move upwards and to the right, which indicates an increase in the maximum output power.

Graph (b) (P-V Curve): This graph shows the P-V curve for a given irradiance level. The curve has a single peak, marked as Pmax, which is the maximum power point the system can extract from the array under those specific conditions. The voltage corresponding to this point is indicated by Vmax. The hatched area below this curve represents the total power that can be obtained from the system at different voltages. The objective of an MPPT system is to always keep the system's operating point at Vmax (and consequently Pmax) to extract the maximum possible power.

2.1. Classification and Review of MPPT Methods

In recent years, a large number of MPPT algorithms have been proposed, with differences in cost, complexity, required sensors, convergence speed, effectiveness range, and hardware implementation. Initially, various MPPT methods will be introduced, and their advantages and disadvantages will be reviewed. These results are based

on articles published in reputable scientific journals and international conferences.

2.1.1. Hill Climbing and Perturb & Observe (P&O) Methods

Hill Climbing and Perturb & Observe (P&O) are common MPPT methods that have received significant attention due to their simple structure. The Hill Climbing method works by introducing perturbations into the converter's operating cycle, which results in disturbances in the voltage and current. In the P&O method, perturbations in the operating voltage of the array lead to an increase or decrease in output power, and by maintaining or reversing the perturbation direction, the system gradually approaches the maximum power point (MPPT) [16, 17]. The P&O algorithm is widely used in PV systems due to its ease of implementation. In this method, by periodically changing the duty cycle, the operating point of the panel is altered, and the power generated by the panel under the new conditions is determined. Then, by comparing the new output power with the previous value, the system selects an appropriate duty cycle to achieve maximum power. The P&O method can be implemented in two forms: two-point and three-point implementations [18].

2.1.2. Two-Point Comparison Method

According to the flowchart in Figure 4, in this method, at each iteration of the main loop, the power (P_{new}) is calculated and then compared with the power from the previous cycle (P_{old}). If $P_{new}>P_{old}$, it indicates that the change made in the duty cycle during the previous step was beneficial. Therefore, in this step, the duty cycle should be adjusted in the same direction (either increased or decreased). However, if $P_{new}<P_{old}$, the duty cycle should be adjusted in the opposite direction compared to the previous step.

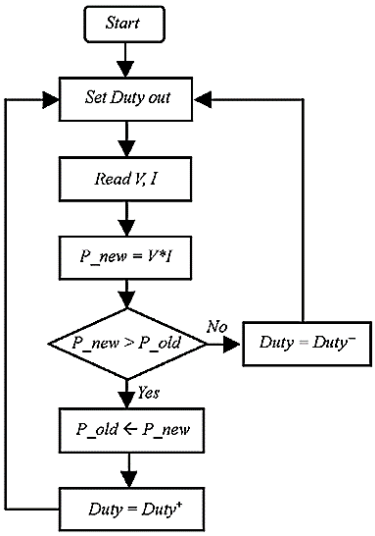

Fig.4. Two-Point Method Algorithm [8].

2.1.3. Three-Point Comparison Method

In this algorithm, three points on the voltage-power curve are compared. These three points are: A (the previous operating point), point B (the point obtained by increasing the duty cycle by one unit), and point C (the point obtained by decreasing the duty cycle by one unit). According to Figure 5, for the power values obtained at these three points, there are 9 different states. Based on the current state, the variable M is updated. If the power at point B is greater than or equal to the power at point A, one unit is added to M; otherwise, M is decreased by one unit. Additionally, if the power at point C is less than the power at point A, one unit is added to M; otherwise, M is decreased by one unit [8].

If the value of M becomes two, point B is chosen as the operating point in the next cycle. However, if the value of M becomes negative two, point C is selected as the operating point in the next cycle. In other cases (M equal to zero, one, or negative one), the system has either reached the maximum power point, or there has been a sudden change in the irradiance on the solar cells, meaning there is no need to adjust the duty cycle. Therefore, the operating point remains at point A. Figure 6 shows the flowchart of the above algorithm.

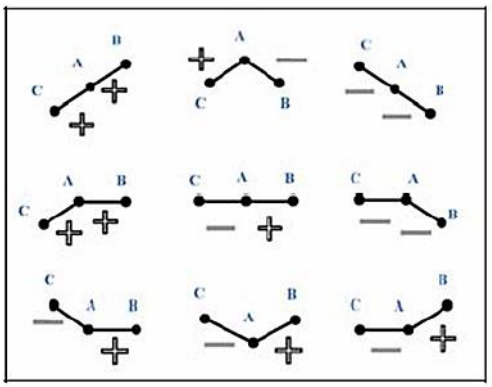

Fig.5. Possible states for the power at the three points.

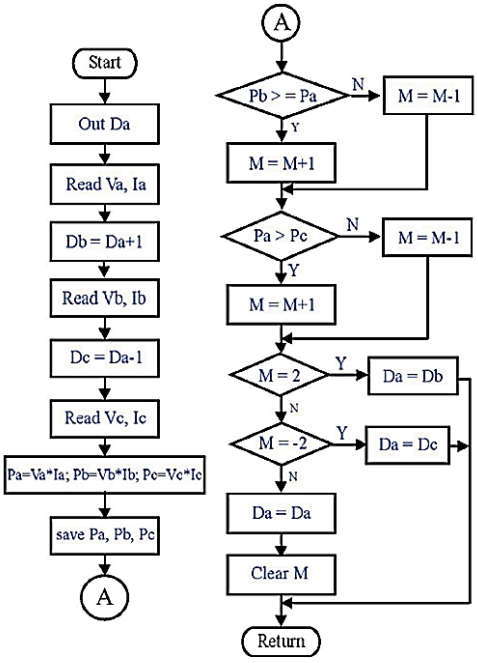

Fig.6. Three-point method algorithm [9].

In the P&O method, if the perturbation size is large, the system oscillates around the MPP (Maximum Power Point), and if the perturbation size is small, the MPP tracking becomes slow. To address this issue, a two-step algorithm is used, where the first step performs rapid tracking, and the second step refines the tracking process. In the first phase, the algorithm quickly adjusts the duty cycle to reach the vicinity of the MPP. Once the system is close to the MPP, the second phase begins, which applies a finer adjustment to minimize oscillations and ensure

more accurate tracking of the MPP.This two-stage approach improves the efficiency of MPP tracking by balancing the speed of convergence and minimizing steady-state oscillations, thereby optimizing performance [4].The advantages of these two methods are low cost, ease of implementation, relatively simple control algorithms, and good MPP tracking. However, their disadvantage is that they fail to track the MPP effectively under rapid changes in temperature and irradiance, which leads to energy losses. To ensure MPP tracking under sudden changes in irradiance, the method uses the P&O algorithm with a three-point comparison. In this approach, the actual power point is compared with the previous two points before a new perturbation signal is generated. This helps to improve the tracking performance during rapid changes in irradiance [8]. In the studies [9, 10], by increasing and optimizing the sampling rate, and in [11] by estimating the array current from the voltage, the need for a current sensor was eliminated, leading to improved efficiency and reduced costs.

2.1.4. Incremental Conductance Method

Another widely used method is the Incremental Conductance (INC) technique, which operates based on the fact that the slope of the power-voltage curve at the Maximum Power Point (MPP) is zero, as shown in Figure 7 [19]. In this method, the sum of the instantaneous conductance $^{I}/_{V}$ and the incremental conductance $^{\Delta I}/_{\Delta V}$ at the MPP is equal to zero. To the right of the MPP, the conductance is negative, and to the left of the MPP, the conductance is positive. Figure 8 shows the algorithm of the incremental conductance method.

If the changes in current and voltage are zero, there is no need to increase or decrease the reference current. If there is no change in current when the voltage change is positive, the reference current should be increased. Similarly, if there is no change in current when the voltage change is negative, the reference current should be decreased. If $I \neq 0$ when $^{\Delta I}/_{\Delta V} = -^{V}/_{I}$, the operating point is at the Maximum Power Point (MPP) for the PV system.

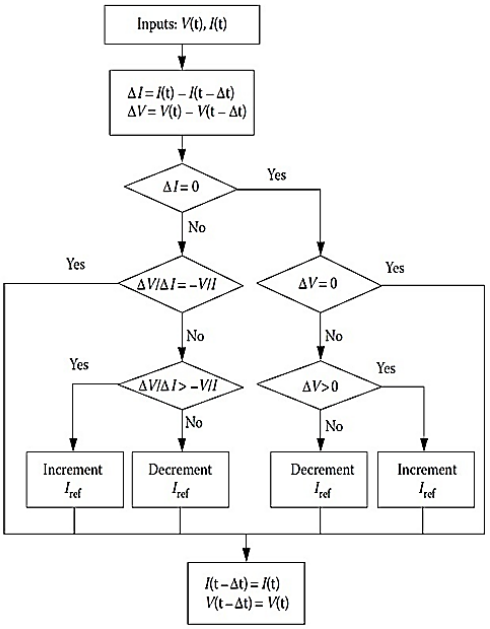

Fig.7. Incremental Conductance Method Algorithm [9].

If $^{\Delta I}/_{\Delta V} \neq -^{V}/_{I}$ and $^{\Delta I}/_{\Delta V} > -^{V}/_{I}$, the reference current should be decreased. However, if $^{\Delta I}/_{\Delta V} \neq -^{V}/_{I}$ and $^{\Delta I}/_{\Delta V} < -^{V}/_{I}$, the reference current should be increased in the direction of tracking the MPP. In practice, due to noise and errors, compensating for the state where $^{\Delta I}/_{\Delta V} = -^{V}/_{I}$ can be difficult. Therefore, this condition can be approximately compensated by $|^{\Delta I}/_{\Delta V} + ^{V}/_{I}| < \varepsilon$, where ε is a small positive value.

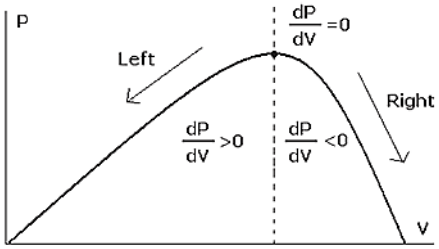

Fig.8. Power-Voltage Curve [9].

$$\begin{cases} \Delta I/\Delta V = -i/V, \text{at MPP} \\ \Delta I/\Delta V > -i/V, \text{left of MPP} \\ \Delta I/\Delta V < -i/V, \text{right of MPP} \end{cases}$$

In the study [20], a two-stage algorithm is used where, initially, the operating point is brought close to the MPP, and then the INC method is applied for precise MPP tracking. In the study [21], the I-V characteristic is divided into two regions using a linear function, and the operating point is brought to a region that includes all possible MPPs under varying environmental conditions. Finally, the INC method is applied for MPP tracking. In studies [22, 23], both instantaneous conductance and incremental conductance are used to generate an error signal e, which is then driven to zero using a PI controller for MPP tracking. In the study [24], incremental resistance with a variable step size is employed, which enhances the speed and accuracy of the steady-state response.

2.1.5. Partial Open-Circuit Voltage (V_{oc}) and Partial Short-Circuit Current (I_{sc}) methods

The Partial Open-Circuit Voltage (Voc) method [25] and Partial Short-Circuit Current (Isc) method [26, 27] are useful and simple methods. However, due to the need for measuring the open-circuit voltage or short-circuit current, these methods require temporarily disconnecting the panel from the system, resulting in a temporary loss of power. To address this issue, the pilot cell method is used. In these methods, there is a linear relationship between the Maximum Power Point Voltage (VMPP) and Maximum Power Point Current (IMPP) with the open-circuit voltage (VOC) and short-circuit current (ISC) of the PV array, which holds under varying irradiance and temperature conditions. The pilot cell method helps in estimating the MPP without needing to disconnect the panel, thus avoiding power loss during measurements [15].

$$V_{MPP} \approx k_1 V_{OC} \quad 0.71 < k_1 < 0.78 \quad (1)$$

$$I_{MPP} \approx k_2 I_{SC} \quad 0.78 < k_2 < 0.92 \quad (2)$$

In this method, K1 and K2 are constants that depend on the characteristics of the PV array. These constants are pre-calculated and determined through observation and

experience for the specific PV array under various irradiance and temperature conditions.

Using the equation and measuring the open-circuit voltage (VOC) of the PV array under no load, the Maximum Power Point Voltage (VMPP) can be calculated by knowing K1. The output terminals of the PV array must be disconnected from the power converter, which results in a temporary loss of power. This is the main drawback of this method. To overcome this issue, pilot cells can be used for measuring VOC. These pilot cells should have similar characteristics to the main PV array under the same irradiance and temperature conditions. For a better approximation of the open-circuit voltage, the P-N junction of diodes produces a voltage that is approximately 75% of VOC, eliminating the need for direct VOC measurement. To adjust the input voltage of the inverter, a closed-loop MPPT voltage control after the DC/DC converter can be implemented.

Figure 9 shows the implementation of the open-circuit voltage (VOC) method based on the MPPT technique. The VMPP can be obtained by measuring the open-circuit voltage from the pilot cells and using equation (1). The measured voltage can then be compared with this value. The duty cycle is determined by a PI controller and applied to the power switch through gate drivers. This ensures that the DC/DC converter forces the PV output voltage to reach VMPP. Due to the approximation in equation (2), the PV array technically never operates exactly at the MPP. Depending on the use of the PV system, this approximation may be acceptable. The implementation of this method is simple and inexpensive because it does not require a complex control system. However, it is not a true MPPT technique. Additionally, K1 is not valid in certain shading conditions, and it must be updated by sweeping the voltage of the PV array. Therefore, implementing this method under shaded conditions is more complex and results in greater power loss.

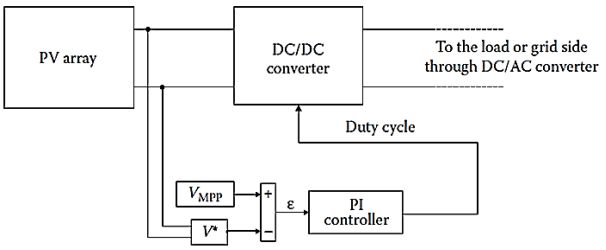

Fig.9. Implementation of Partial Open-Circuit Voltage Based on MPPT [13].

Figure 10 shows an example of implementing the short-circuit current based on the MPPT technique. IMPP can be obtained by measuring the short-circuit current from the pilot cells and using equation (3). The measured current can then be subtracted from this value to determine the error, which is fed into the PI controller. The duty cycle is calculated by the PI controller and applied to the power converter through gate drivers. Thus, the DC/DC converter forces the current drawn from the PV output to reach IMPP. Measuring ISC during operation is very difficult because the PV array must be short-circuited . To measure ISC , the PV array can be short-circuited using a current sensor and an additional switch in the power converter, which increases the number of components and the cost. Furthermore, this causes additional power losses due to the short circuit.

Additional pilot cells can be used to measure the short-circuit current , which have the same characteristics as the main PV array . In this method, the MPP never exactly matches, as suggested by equation 2-3, since it is an approximation of IMPP. To ensure accurate tracking of MPP in the presence of multiple peaks, the PV array can be periodically swept from open-circuit to short-circuit to update the value of K2. In general, DSP is used to implement the partial ISC method based on MPPT for PV systems.

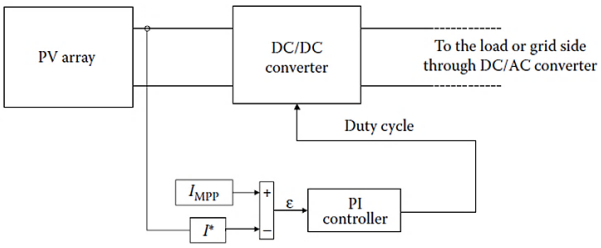

Fig.10. Implementation of Partial Short-Circuit Current Based on MPPT [13].

2.1.6. Fuzzy Logic Control Method

With advancements in microcontroller and DSP technologies, attention to the applications of MPPT in fuzzy logic control has increased. [28, 29] The advantages of fuzzy controllers include their ability to handle imprecise and nonlinear inputs, the lack of necessity for an accurate mathematical model, fast convergence, and minimal oscillation at the MPP. The capabilities of fuzzy systems include online maximum power point tracking, robustness against variations in irradiation and temperature, and the absence of a need for external sensors to measure irradiation intensity and temperature [30]. Fuzzy logic control is based on three stages:

1. Fuzzification 2. Rule Determination Based on a Lookup Table 3.Defuzzification

The fuzzification stage converts the input variable into a linguistic variable based on a membership function, as shown in Figure 11. In this case, there are five fuzzy levels: NB (negative big), NS (negative small), ZE (zero), PS (positive small), and PB (positive big).

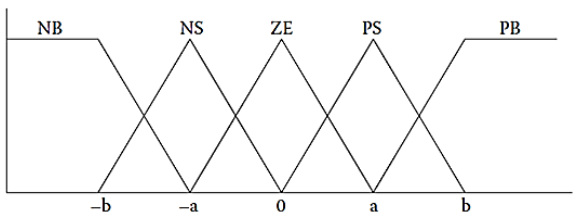

Fig.11. Fuzzification is the process of converting the input variable into a linguistic variable [30].

To enhance accuracy, a greater number of fuzzy levels can be used. The error (E) and the change in error (Delta E) are the inputs to the fuzzy logic-based MPPT controller. (E) and (Delta E) can be calculated based on user preferences. Since (dP/dV) in MPPT approaches unity, an approximation of Equation (3) can be utilized [5].

$$E(n) = \frac{P(n)-P(n-1)}{V(n)-V(n-1)} \quad (3)$$

$$\Delta E(n) = E(n) - E(n-1) \quad (4)$$

Alternatively, the error signal can be calculated as follows [5]:

$$e = \frac{I}{V} + \frac{dI}{dV} \quad (5)$$

In general, the output of the fuzzy logic is the change in (Delta D) of the power converter. This change in (Delta D) can be searched in a rule table like Table 1. Immediately after (E) and (Delta E) are calculated, they are converted into linguistic variables. Various combinations of error (E) and its changes (Delta E) can be used as linguistic variables and assigned to (Delta D). For a boost converter, Table 1 can be used for this purpose. For example, if the operating point is far to the right of the MPP and (E) is NB and (Delta E) is ZE, then a large decrease in (Delta D) is required to reduce the voltage. (Delta D) must be set to NB to reach the MPP.

Table 1. Fuzzy Rule Table [24].

ΔE	NB	NS	ZE	PS	PB
E					
NB	ZE	ZE	NB	NB	NB
NS	ZE	ZE	NS	NS	NS
ZE	NS	ZE	ZE	ZE	PS
PS	PS	PS	PS	ZE	ZE
PB	PB	PB	PB	ZE	ZE

The output of the fuzzy controller is the conversion of a linguistic variable into a numerical variable, and a membership function, as shown in Figure 12, is used for the fuzzy level in question. Through fuzzification, the controller generates an analog output signal, which can be converted into a digital signal to control the power converter of the MPPT system. Figure 12 shows a simple example of implementing fuzzy logic control based on MPPT. The measured voltage and power, E and ΔE, are calculated from Equations (3) and (4). These values are then evaluated and simulated using the fuzzy rules from Table 1. The output of the fuzzy rules, based on the table, necessitates a change in ΔD. In the defuzzification stage, the numerical value of ΔD is determined by converting the linguistic values. Finally, the required switching signal to transfer power to MPPT is applied through an analog-to-digital converter and a gate driver.

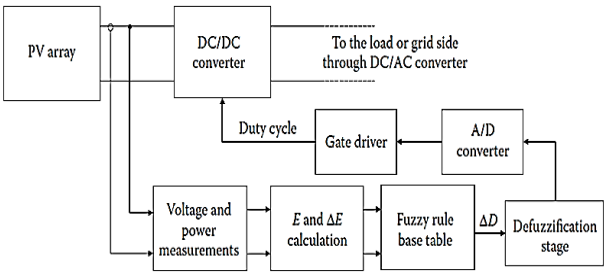

Fig.12. Implementation of Fuzzy Logic Control Based on MPPT [6].

Under different weather conditions, the fuzzy logic controller shows good performance in MPPT applications. On the other hand, the effectiveness of the fuzzy logic controller depends on the accuracy of error calculation, its variation, and the rules developed in the base table by the user. For better efficiency, the functions and rules in the base table can be continuously updated or adjusted for optimal performance, similar to an adaptive fuzzy logic controller. In this way, rapid convergence to MPPT and minimal oscillations around the MPPT can be achieved. Additionally, tracking performance depends on the type of membership function [31].

The flowchart in Figure 12 illustrates the implementation of a FLC for MPPT. The details of each step in this flowchart are analyzed below.

1-PV Array: This section is the primary source of energy generation. The voltage and power generated by the PV array are measured and used as the main inputs for the fuzzy control system.

2-Voltage and Power Measurements: This stage continuously measures the instantaneous voltage and power of the PV array. These measurements form the primary basis for the subsequent calculations.

3-E and ΔE Calculation: In this block, the two main inputs for the fuzzy controller are calculated:

E (Error): This value represents the current position of the operating point relative to the Maximum Power Point (MPP). It is obtained from the formulas mentioned in the paper, such as dP/dV.

ΔE (Change in Error): This value indicates the speed and direction of the operating point's movement. It is calculated by comparing the current error with the error from the previous step.

4-Fuzzy Rule Base Table: This section is the heart of the fuzzy controller. Based on the linguistic values of the inputs E and ΔE, a linguistic output value for ΔD (change in duty cycle) is selected from the rule table (e.g., Table 1). This table contains "If-Then" rules that embed expert experience and knowledge. For example: "If E is Negative Big (NB) and ΔE is Zero (ZE), then ΔD should be Negative Big (NB)."

5-Defuzzification Stage:This stage converts the linguistic output value (such as NB, NS, etc.) obtained from the fuzzy rule base into a precise numerical value. Various methods can be used for defuzzification, such as the Center of Gravity (CoG) or the Mean of Maxima (MoM). The result of this stage is the numerical value of ΔD, which is then applied to the duty cycle.

6-Analog to Digital (A/D) Converter: This converter transforms the analog voltage and current signals measured from the PV array into a digital signal. This digital signal is then processed by the processor or microcontroller on which the fuzzy controller is implemented.

7-Gate Driver: This block receives the digital control signal from the fuzzy controller and converts it into a suitable signal for the power switches in the DC/DC converter. Its main function is to provide the necessary current and voltage to quickly and effectively activate and deactivate the switches.

8-DC/DC Converter: This converter adjusts the PV array's output voltage based on the duty cycle received from the controller. Its purpose is to shift the system's operating point so that the array's voltage and current are positioned at the maximum power point.

2.1.7. Parasitic Capacitor Method

The parasitic capacitor method is based on adding parasitic capacitance in the calculations of the INC algorithm, which uses the ripple caused by switching to

create disturbance in the array. [32] In this method, the ripple voltage and power of the array are calculated using boosting filters, and then the MPP tracking is performed by calculating the inductance of the array. Due to the small capacitive value in a PV array, this method is only used for large arrays with multiple arrays connected in parallel.

2.1.8. Ripple-Dependent Control Method

The Ripple-Dependent Control (RCC) method uses the inherent ripple of the system for Maximum Power Point (MPP) tracking. Due to the switching action of the power converter, voltage and current ripples are present on the PV array, causing the output power of the PV array to have a ripple. RCC controllers are responsible for linking the time derivative of power with the time derivatives of current and voltage, thus zeroing out the power slope to reach the MPP [32].

If the voltage or current increases and the power also increases, then the operating point is below the MPP. Conversely, if the voltage or current increases and the power decreases, the operating point is above the MPP. Based on these observations, it can be stated that the time derivatives of power with respect to voltage pv or current pi are negative to the right of the MPP, positive to the left, and zero at the MPP. If ΔD of the boost converter increases, the inductor current also increases, although the PV array decreases. This inductor current is also the output current of the PV array. Therefore, the input control ΔD can be expressed as follows [7]:

$$d(t) = -k_3 \int \dot{p}\dot{v}dt \quad (6)$$

$$d(t) = k_3 \int \dot{p}\dot{i}dt \quad (7)$$

Where K3 is a positive constant. In the RCC method, if the duty cycle is controlled by Equations (6) or (7), it continuously tracks the MPP. Taking derivatives of current, voltage, and power in Equations (6) and (7) is usually computationally challenging. Therefore, measuring voltage and current using AC coupling from the PV array can be used. The calculation of the derivatives from the voltage and current using AC coupling becomes easier because they require phase information.

Another method is to use a high-pass filter with a cutoff frequency higher than the ripple frequency to estimate the derivatives. The inductor voltage can be used to calculate the derivative in Equation (7) since it is proportional to the current derivative. The internal resistance of the inductor and core loss have a significant effect because the time constant of the inductor is greater than the switching delay of the power converter. Considering the phase shift of the parasitic capacitance of the PV array at high switching frequencies, Equation (6) might not lead to effective MPPT in the system. However, the relationship between power and voltage, as given in Equation (6), is hardly affected by the parasitic capacitance.

Even under varying irradiance, RCC can accurately track the MPP with a fast response. The switching frequency of the power converter and the gain of the RCC circuit are the factors that limit the MPPT response time. The implementation of RCC is feasible since it does not require specific characteristics of the PV array.The advantages of this method for continuous MPP tracking with duty cycle control include: no need for prior knowledge of the PV array characteristics, and the convergence time being limited by the switching frequency of the converter and the gain of the RCC circuit.

2.1.9. Current Sweep Method

In the current sweep method, by using a sweep waveform for the current of the PV array and updating the curve at a fixed time interval, VMPP can be calculated from the characteristic curve within that time interval [30]. This method is particularly useful when the power consumption of the power tracking unit in the PV system is low.

2.1.10. DC-Link Capacitor Control

In some cases, PV systems need to be connected to the AC power grid. In such cases, a specific MPPT method called DC-Link Capacitor Control can be used, the overall structure of which is shown [31,32].

This method helps to regulate the voltage across the DC-link capacitor to ensure stable operation and to manage the power conversion effectively when interfacing with the AC grid. The DC-Link Capacitor acts as a key component in maintaining the system's voltage balance, which is crucial for the proper functioning of both the PV array and the grid connection.

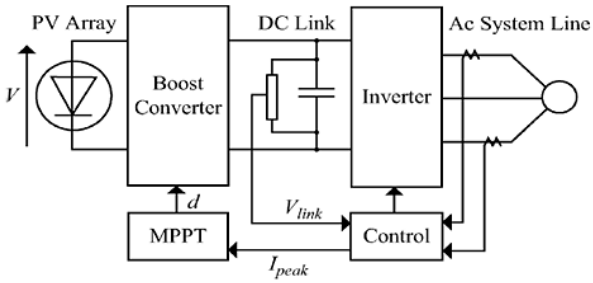

Fig.13. The overall structure of the DC-Link Capacitor Control method [27].

The duty cycle of an ideal boost converter in steady-state operation is obtained by Equation (8) [27] :

$$d = 1 - \frac{V}{V_{link}} \quad (8)$$

Where V is the input voltage across the power converter, and VLink is the voltage across the DC link. If VLink is kept constant, the photovoltaic output power can be controlled by adjusting the input current of an inverter. The VLink voltage can remain constant as long as the required power by the converter does not exceed it, and the maximum available power from the PV array is used when the current is increasing. Otherwise, VLink will decrease. The current control command (IPeak) from the inverter is at its maximum, and the PV array operates to the right of the MPP point. However, compared to methods where power is identified directly, this method has lower accuracy, since the DC voltage control loop response directly impacts its own response. If VLink is kept constant, an increase in the inverter current increases the output power from the boost converter, which in turn increases the input power from the PV array. The control procedure can easily be implemented with analog amplifier operators and decided by a logical unit.

The advantages of this method are the lack of need for array power calculation, simplicity of the control design, and implementation with analog circuits.

2.1.11. Maximizing load voltage or current

In the method of maximizing load voltage or current, if the load is a voltage source, the load current is maximized, and if the load is a current source, the load voltage is maximized. If the load is nonlinear, maximum output power is achieved by maximizing the load current or voltage, provided the impedance is not negative [33]. In many PV systems, a battery is used as the primary load or as a backup. Since a battery can be assumed as a voltage source load type, the load current can be used as the control variable. The advantage of this method is the use of only one sensor.

2.1.12. The method of feedback control using $^{dP}/_{dI}$ or $^{dP}/_{dV}$

In the control feedback method, the slope of the power curve, $^{dP}/_{dI}$ or $^{dP}/_{dV}$, is first calculated. Then, by applying it with feedback to the converter, the slopes are nullified using multiple controls, and the MPP point is obtained [33].

2.1.13. MPPT control based on linearized I-V characteristics

The I-V characteristic is a function of voltage, insulation level, and temperature. From these properties, some important features for designing an MPPT controller can be explained as follows.

The PV array consists of two operational parts. In an I-V characteristic curve, one of these parts is the constant voltage section, and the other is the constant current section. Therefore, the I-V characteristics can be approximated as a linear function of both sections, such that:

$$I_P = -mV_P + b \quad (9)$$

Where m is the output conductivity of a PV array. m is small in the constant current section, so the PV array presents a large negative output impedance. On the other hand, a small negative output impedance is presented in the constant voltage section. The same linearization can be performed for both sections by varying m and the coefficients b. Figure 14 shows a typical I-V curve with a linear approximation of the two sections.

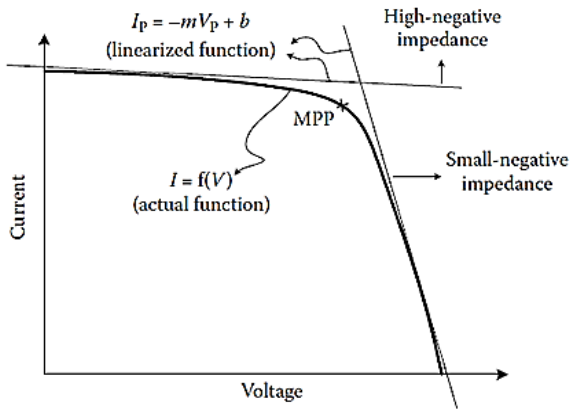

Fig.14. A typical I-V curve with linear approximation [12].

The MPP occurs at the knee of the characteristic curve, where (VP=VPM). The slope in the constant current section is positive (VP<VPM), whereas the slope in the constant voltage section is negative (VP>VPM). Using Equation (10), $^{dPPV}/_{dVP}$ is given by:

$$\frac{dP_{PV}}{dV_P} = I_P - mV_P \quad (10)$$

In order to move the operating point toward a point with zero slope, if the PV array is controlled by current, then IP should be decreased for a positive slope and increased for a negative slope. Therefore, the MPP can track the operating point toward a point with zero slope. A DC/DC boost converter can be used for current control [12].

$$I_P = I_{cap} + I_C = C_i \frac{dV_P}{dt} + I_C \quad (11)$$

In steady-state, (IP) is equal to the converter current (IC). Therefore, the operating point can move towards the MPP by adjusting (IC). An MPPT controller for tracking the MPP using current mode control is proposed, as shown in Figure 15. This MPPT controller and current mode controller are based on the above properties in Equation (11).

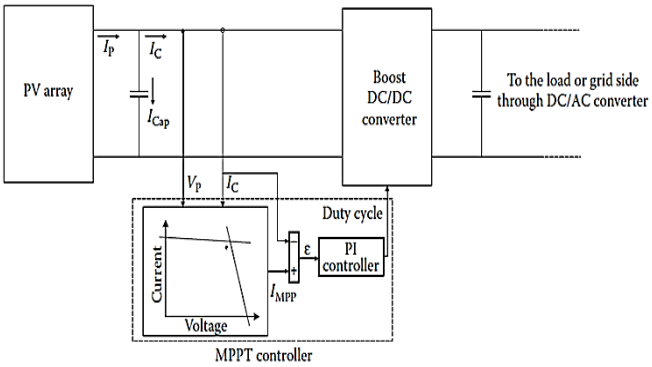

Fig.15. The MPPT controller and current mode controller [29].

In this controller, the voltage and current of the PV array are first measured, and power and slope are computed. In steady-state, the PV current is equal to the converter current. Therefore, based on the sign of the slope $(^{dP_{PV}}/_{dV_P})$, the reference current IMPP is increased or decreased to move the operating point towards zero.

2.1.14. Gravitational Search Algorithm (GSA)

The Gravitational Search Algorithm (GSA) is a metaheuristic optimization algorithm inspired by Newton's law of universal gravitation. In this algorithm, search agents are treated as celestial bodies that interact with each other through gravitational force. The algorithm aims to find the optimal solution for optimization problems. In GSA, each agent (candidate solution) is considered a mass. The better a solution is, the greater its mass. According to the law of gravity, heavier masses exert a stronger force on lighter masses and attract them. This attraction causes the lighter agents to move toward the heavier ones. The best agent (the heaviest mass) in each iteration has the strongest gravitational pull, causing all other agents to move toward it. This process ultimately leads to the convergence of all agents (solutions) toward the best mass (the optimal solution) within the search space. In this method, the main parameters are defined as follows:

Population Size (N): The number of search agents (masses) participating in the algorithm. A larger population size increases the probability of finding the optimal solution but also increases computation time.

Number of Iterations (T): The number of times the algorithm repeats for optimization. Increasing the number

of iterations improves the solution's accuracy but also increases computation time.

Mass (M): The mass of each agent is calculated using a fitness function. An agent with a better fitness value will have a greater mass.

Gravitational Constant (G): This parameter decreases over time. Initially, its value is high to allow agents to move rapidly throughout the search space (exploration). Its value then decreases over time to increase the accuracy of convergence to the optimal solution (exploitation).

Fitness Function Formulation

In optimization problems, the fitness function is formulated as follows [39]:

For minimization problems:

$$fit_i(t) = f(x_i(t)) \quad (12)$$

For maximization problems:

$$fit_i(t) = f(x_i(t)) \quad (13)$$

Then, the best and worst fitness values within the population are determined in each iteration:

For minimization:

$$Best(t) = min_{j\epsilon\{1,..N\}} fit_j(t) \quad (14)$$

For maximization:

$$Worst(t) = max_{j\epsilon\{1,..N\}} fit_j(t) \quad (15)$$

The mass of each agent is then normalized using these values. The following formulas are typically used for this normalization:

$$m_i(t) = \frac{fit_i(t) - Worst(t)}{Best(t) - Worst(t)} \quad (16)$$

The normalized mass Mi(t) is then calculated for each agent:

$$M_i(t) = \frac{m_i(t)}{\sum_{j=1}^{N} m_j(t)} \quad (17)$$

3. Simulation of Maximum Power Point Tracking (MPPT) using the Gravitational Search Algorithm (GSA)

In this section, to test and validate the proposed method, the simulation of the introduced algorithm for tracking the maximum power point (MPP) of a photovoltaic system connected to the grid will first be performed under uniform irradiation and temperature conditions. Then, the simulation of the proposed algorithm under partial shading conditions will be addressed.

3.1. Evaluation of the proposed algorithm under uniform irradiation and temperature conditions.

In this section, the performance of the proposed algorithm for tracking the maximum solar power point under uniform irradiation and temperature conditions is examined. The simulated circuit for this issue is shown in Figure (16).

In Figure (16), the various components of the discussed circuit are shown, and the information related to the solar panel is provided in Table (2). As observed in Figure (16), in this circuit, the proposed GSA algorithm first determines the voltage corresponding to the maximum solar power point at each time step of the simulation after receiving the irradiation and temperature data. After that, the duty cycle of the circuit's switching is adjusted by the fuzzy controller so that the output voltage of the solar panel matches the voltage suggested by the GSA algorithm. In this case, it can be expected that the maximum solar power point is accurately tracked. As shown in Figure (17), the maximum output power of the photovoltaic system is well-tracked in both the DC and AC sections as solar irradiation and ambient temperature change. Additionally, Figure (18) shows the graph of the output voltage and current variations of the photovoltaic system at the grid connection point. As observed in this figure, as the output power of the photovoltaic system changes, the voltage amplitude and the output current change, indicating the proper and optimal performance of the fuzzy controller in maintaining the DC link voltage and the inverter's AC control circuit at the grid connection point.

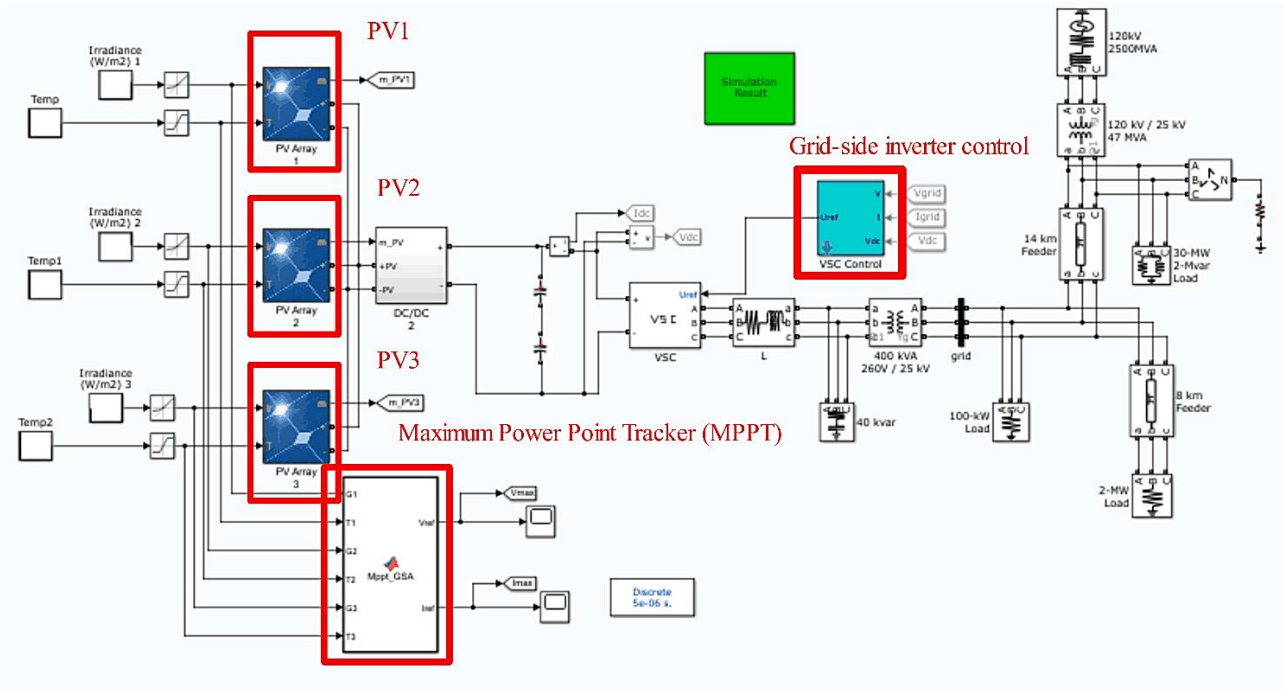

Fig.16. Schematic of the MPPT circuit under uniform irradiation and temperature conditions.

Furthermore, Figure (19) presents the power variations of each part of the photovoltaic system under uniform changes in irradiation and temperature. As shown in this figure, due to the uniform irradiation and temperature input in each section, the output power of all three sections is always equal, and their sum matches the maximum tracked power.

Table 2. Characteristics of Silicon Solar Cell Array at 25°C.

Temperature Coefficient of Current	$\alpha = 0.002086[A/C^{\circ}]$
Temperature Coefficient of Voltage	$\beta = 0.0779[V/C^{\circ}]$
Reverse Saturation Current	$I_s = 0.5 \times 10^{-4}[A]$
Short-Circuit Current	$I_{SC} = 2.926[A]$
Cell Resistance	$R_S = 0.0277[\Omega]$
Cell Material Coefficient	$\lambda = 20.41[V^{-1}]$

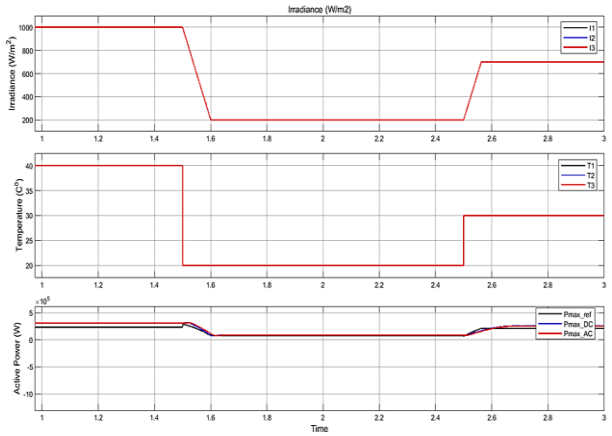

Fig.17. MPPT Tracking and Corresponding Voltage Under Uniform Irradiance and Temperature Conditions.

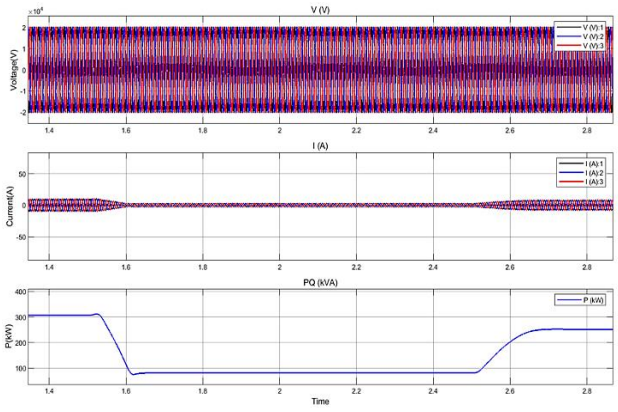

Fig.18. The diagram of variations in voltage, current, and active power output of the photovoltaic system in the AC section.

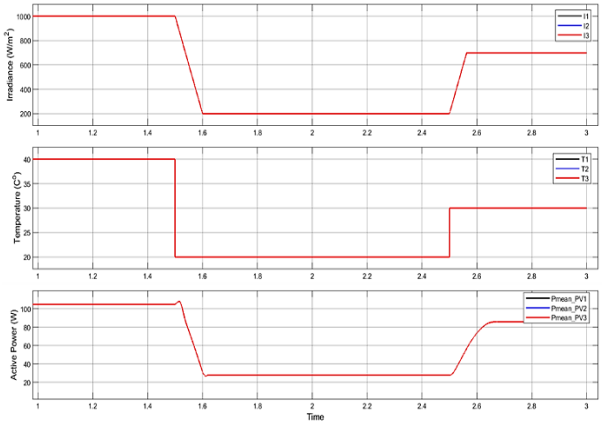

Fig.19. The variation in output power of each section of the photovoltaic system under uniform irradiance and temperature conditions.

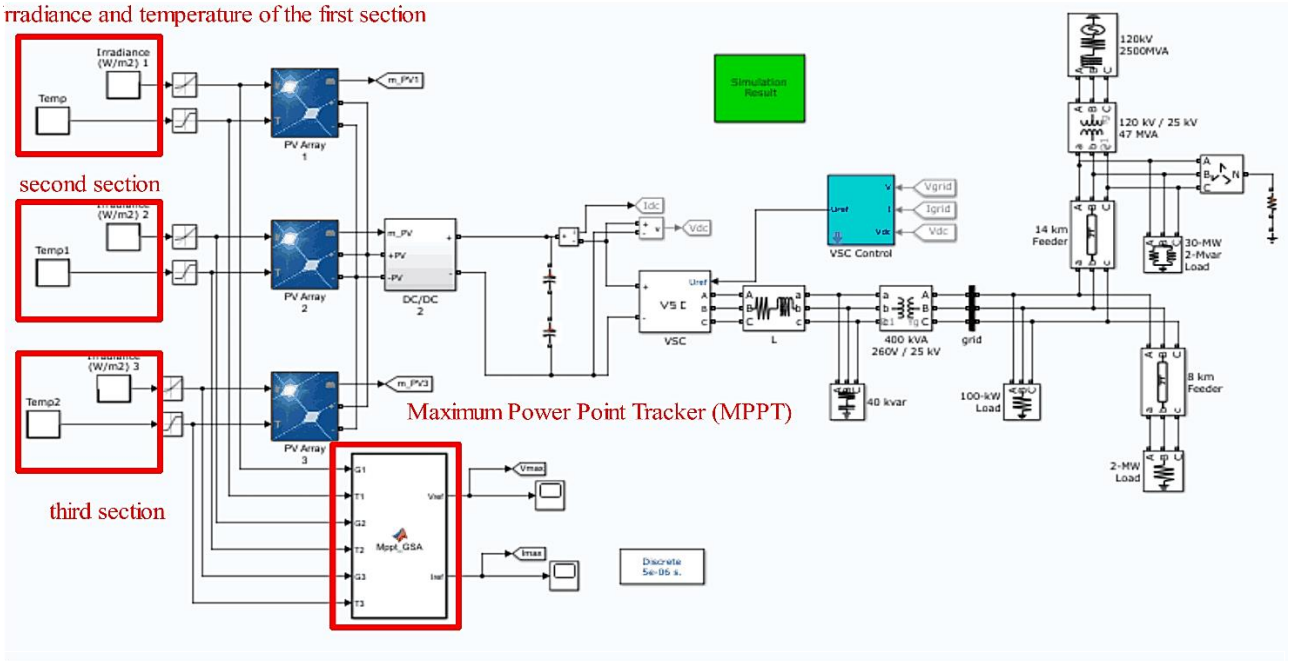

Fig.20. The electrical circuit for testing and validating the proposed method.

3.2. Evaluation of the proposed algorithm under partial shading conditions

Consider the circuit shown in Figure (20), which has been simulated in the MATLAB Simulink environment.

As shown in Figure (20), the solar module in the electrical circuit consists of three different sections, each exposed to different irradiance and temperature conditions. The characteristics of these panels are presented in Table (2). In this section, the proposed algorithm's testing and validation for tracking the maximum solar power point (MPPT) in a solar module consisting of three sections under partial shading conditions will be discussed. To assess the performance speed and effectiveness of the proposed algorithm in tracking the MPPT point during partial shading conditions, as shown in Figure (21), partial shading conditions for the three sections of the solar panel are changed. As observed in Figure (21), with the rapid changes in partial shading conditions, the proposed algorithm quickly and accurately tracks the output voltage and power of the solar panel towards the point of maximum solar power. In this regard, the proposed GSA algorithm determines the operating voltage corresponding to the maximum power point at any moment, and the fuzzy neural controller adjusts the DC link voltage by switching the boost converter to the voltage that corresponds to the maximum power.

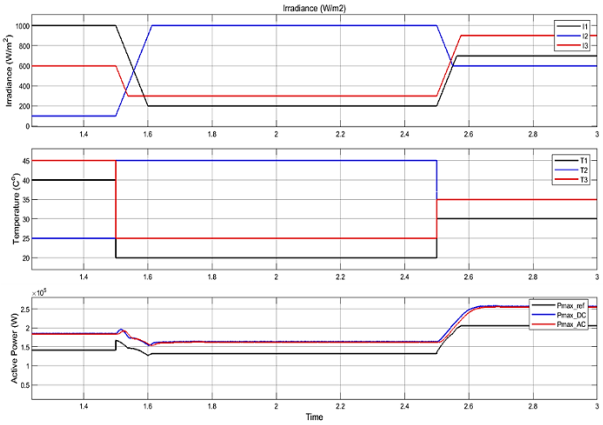

Fig.21. Graph of rapid changes in solar radiation and ambient temperature for three different sections of the solar panel and changes in power in the DC and AC sections.

Similar to before, in Figure (22), the graph of voltage and current variations of the photovoltaic system at the point of connection to the grid is shown. As observed in this figure, with the change in the output power of the photovoltaic system, the voltage range and output current change, indicating the proper and optimal performance of the fuzzy controller in maintaining the DC link voltage and the AC inverter control circuit at the point of connection to the grid. Additionally, in Figure (23), the graph of power changes in each section of the photovoltaic system with identical radiation and temperature variations for each section is shown. As seen in this figure, due to the differences in radiation and input temperature in each section, the output power of each of the three sections is always different, but the sum of them equals the maximum power tracked.

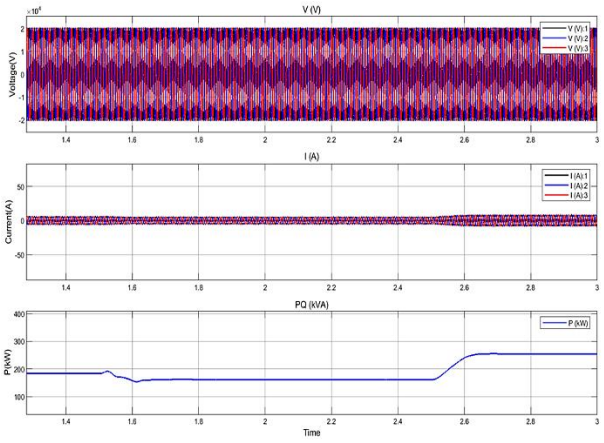

Fig.22. The graph of voltage, current, and output power variations of the solar panel in the AC section and the connection point to the grid under conditions of rapid changes in solar irradiance and ambient temperature.

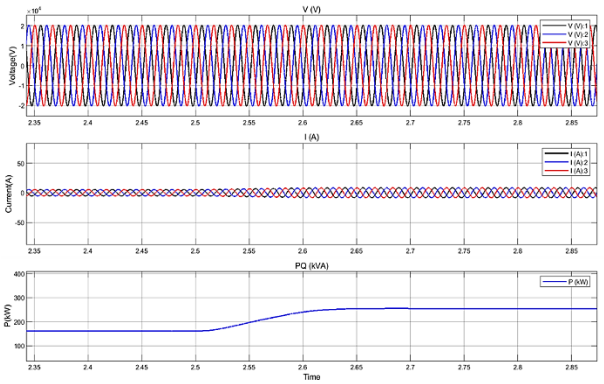

Fig.23. The graph of voltage, current, and output power variations of the solar panel in the AC section and the connection point to the grid under conditions of rapid changes in solar irradiance and ambient temperature.

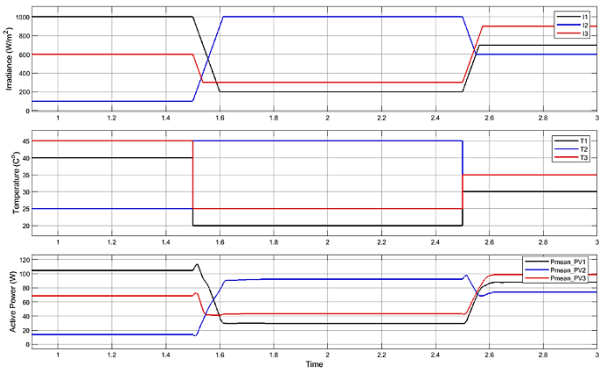

Fig.24. The output power variations of each part of the photovoltaic system under partial shading conditions.

4. Discussion

This paper presents a MPPT method using the GSA for grid-connected microgrid photovoltaic (PV) systems under PSC. The method focuses on efficiently extracting maximum power even in the presence of multiple local peaks on the power-voltage (P-V) curve, which are caused by partial shading. Simulations show that GSA performs well in tracking the MPP under both uniform irradiation and partial shading conditions. As a standalone metaheuristic algorithm, GSA offers a simpler implementation compared to more complex hybrid

methods like Neuro-Fuzzy-GSA [34] or HPSO-GSA [42]. Ref 40 is used as the base reference for this paper because both articles use GSA in combination with a fuzzy controller to regulate the DC-DC converter and achieve nearly identical results under variable partial shading conditions. Furthermore, the PV array specifications used in the simulations (as shown in Table 2 in both papers) are exactly the same. Based on the simulation graphs presented in ref 40, the convergence time of the proposed algorithm can be analysed across different scenarios. The most important scenario for evaluating speed and accuracy is the analysis of the graph under variable temperature and partial shading conditions, as it simulates a more realistic situation. In this scenario, three sections of the PV array are subjected to irradiances of 1000, 850, and 750 W/m² and temperatures of 30, 28, and 25 °C, respectively.

Figure 13 [40] shows that the method can track the maximum power (approximately 680 W) in about 0.2 seconds with high accuracy. The graph of the tracked power for the proposed method under variable temperature and partial shading conditions (Figure 21) shows that this method has a faster response of 100 ms. For comparison, the PSO method in [38] has an MPPT tracking speed of 0.53 seconds, which is slower than the proposed method.

Conventional methods such as P&O [37] and INC [44] suffer from steady-state oscillations, low convergence speed, and an inability to track the Global Maximum Power Point (GMPP) under partial shading conditions. If the perturbation size in the P&O method is large, the system will oscillate around the MPP. If the perturbation size is small, the MPPT tracking speed slows down. These methods fail to track the MPP under rapid changes in temperature and solar irradiance, leading to energy losses. They consistently get trapped in Local Maximum Power Points (LMPPs) and are unable to track the GMPP. The Gravitational Search Algorithm (GSA), as a metaheuristic algorithm, inherently overcomes these limitations by providing global search capability and better management of multiple peaks.

Ref [43] shows that the P&O and IC methods reduce efficiency to 68.20% and 68.15% (Scenario 4), respectively, because they get trapped in LMPPs. Due to their offline nature, methods like OCV [37] and SCC [44] have low accuracy and efficiency. Ref [37] reports that OCV efficiency is approximately 86% and SCC is approximately 89%. The GSA method, which is aimed at tracking the GMPP under PSC, has higher efficiency compared to these methods.

5. Conclusion

In this study, the performance of the Gravitational Search Algorithm (GSA) for Maximum Power Point Tracking (MPPT) in a photovoltaic system connected to a microgrid under partial shading conditions was evaluated. The results demonstrated that GSA effectively improves the MPPT's efficiency, overcoming the challenges posed by partial shading. By accurately locating the global maximum power point (GMPP), the GSA-based MPPT method ensured enhanced power extraction and system stability. The graph of the tracked power for the proposed method in this paper, under variable temperature and partial shading conditions (Figure 21), showed that this method has a faster response (100ms) compared to the GSA method found in [40]. Conventional methods like P&O and INC suffered from steady-state oscillations, low convergence speed, and an inability to track the Global Maximum Power Point (GMPP) under partial shading conditions. These methods failed to track the MPP under rapid changes in temperature and solar irradiance, which led to energy losses. They also consistently got trapped in Local Maximum Power Points (LMPPs) and could not track the GMPP. GSA, as a metaheuristic algorithm, inherently overcomes these limitations by providing a global search capability and better management of multiple peaks. However, as a standalone method, GSA may be slower in terms of convergence speed and settling time compared to more advanced metaheuristic methods such as HPSO-GSA, PSODTVAC, or BOA. This highlights the necessity of combining GSA with other methods (e.g., Neuro-Fuzzy GSA in [34] and [40] or HPSO-GSA in [42]) to improve its performance.

Future work may focus on further optimizing the GSA and combining it with other advanced control strategies to improve system performance in real-world applications.

6. References

[1] T.F. Wu, C.H. Chang, Z.R. Liu, T.H. Yu, “Single-stage converters for photovoltaicpowered lighting systems with MPPT and charging features”, In Proc. IEEEAPEC, pp. 1149–1155, 1998.

[2] A.M. De Broe, S. Drouilhet, V. Gevorgian, “A peak power tracker for small windturbines in battery charging applications”, IEEE Transactions on Energy Conversion, vol. 14, no. 4, pp. 1630–1635, 1999.

[3] A.B.G. Bahgat, N.H. Helwab, G.E. Ahmadb, E.T. El Shenawyb, “Maximum powerpoint tracking controller for PV systems using neural networks”, Renewable Energy, vol. 30, pp. 1257–1268, 2005.

[4] V. Salas, E. Olıas, A. Barrado, A. La zaro, “Review of the maximum power pointtracking algorithms for stand-alone photovoltaic systems”, Solar Energy Materials & Solar Cells, vol. 90, pp. 1555–1578, 2006.

[5] T. Esram, P.L. Chapman, “Comparison of photovoltaic array maximum power point tracking techniques”, IEEE Transactions on Energy Conversion, vol. 22, no. 2, pp. 439-449, 2007.

[6] M.G. Villalva, J.R. Gazoli, E.R. Filho, “Comprehensive approach to modeling andsimulation of photovoltaic arrays”, IEEE Transactions on Power Electronics, vol. 24, no. 5, pp. 1198–1208, 2009.

[7] J.J. Schoeman, J.D. Van Wyk, “A simplified maximal power controller forterrestrial photovoltaic panel arrays”, In IEEE power electronics specialists conference PESC ‘82 Record, New York, NY, pp. 381-387, 1982.

[8] M. Abou El Ela, J. Roger, “Optimization of the function of a photovoltaic array using a feedback control system”, Solar Cells, vol. 13, pp. 107–119, 1984.

[9] G.W. Hart, H.M. Branz, C.H. Cox, “Experimental tests of open-loop maximum power-point tracking techniques”, Solar Cells, vol. 13, pp. 185–195, 1984.

[10] M. Andersen, B. Alvsten, “200 W low cost module integrated utility interface for modular photovoltaic energy systems”, In Proceedings of IECON ‘95, vol. 1, pp. 572–577, 1995.

[11] J.H.R. Enslin, M.S. Wolf, D.B. Snyman,

W. Swiegers, “Integrated photovoltaic maximum power point tracking converter”, IEEE Transactions on Industrial Electronics, vol. 44, pp. 769–773, 1997.
[12] J.F. Schaefer, L. Hise, “An inexpensive photovoltaic array maximum power point tracking DC-to-DC converter”, Number NMSEI/TN-84-1 New Mexico Solar Energy Institute, Las Cruces, New Mexico, 1984.
[13] Z. Salameh, F. Dagher, W. Lynch, “Step-down maximum power point tracker for photovoltaic systems”, Solar Energy, vol. 46, no. 5, pp. 279–282, 1991.
[14] S.M. Alghuwainem, “Matching of a dc motor to a photovoltaic generator using a step-up converter with a current-locked loop”, IEEE Transactions on Energy Conversion, vol. 9, pp. 192–198, 1994.
[15] N. Mutoh, T. Matuo, K. Okada, M. Sakai, “Prediction-data-based maximum power-point-tracking method for photovoltaic power generation systems”, In Proc. 33rd Annu. IEEE Power Electron. Spec. Conf., pp. 1489–1494, 2002.
[16] M.A.S. Masoum, H. Dehbonei, E.F. Fuchs, “Theoretical and experimental analyses of photovoltaic systems with voltage and current-based maximum power-point tracking”, IEEE Transactions on Energy Conversion, vol. 17, no. 4, pp. 514–522, 2002.
[17] T. Noguchi, S. Togashi, R. Nakamoto, “Short-current pulse-based maximum power-point tracking method for multiple photovoltaic-and-converter module system”, IEEE Transactions on Industrial Electronics, vol. 49, no. 1, pp. 217–223, 2002.
[18] S. Yuvarajan, S. Xu, “Photovoltaic power converter with a simple maximum power-point-tracker”, In Proc. 2003 Int. Symp. Circuits Syst., pp. III-399–III-402, 2003.
[19] C. Zhang, D. Zhao, J. Wang, “A novel two-mode MPPT method for photovoltaic power generation system”, In IEEE 6th International Conference on Power Electronics and Motion Control, pp. 2100-2102, 2009.
[20] C. Yang, C. Hsieh, F. Feng, K. Chen, “Highly efficient analog maximum power point tracking (AMPPT) in a photovoltaic system”, IEEE Transactions on Circuits and Systems I: Regular Papers, vol. 59, no. 7, pp. 1568-1577, 2012.
[21] T. Hiyama, S. Kouzuma, T. Imakubo, “Identification of optimal operating point of PV modules using neural network for real time maximum power tracking control”, IEEE Transactions on Energy Conversion, vol. 10, no. 2, pp. 360–367, 1995.
[22] T. Hiyama, K. Kitabayashi, “Neural network based estimation of maximum power generation from PV module using environmental information”, IEEE Transactions on Energy Conversion, vol. 12, pp. 241–247, 1997.
[23] F. Giraud, Z.M. Salameh, “Analysis of the effects of a passing cloud on a gridinteractive photovoltaic system with battery storage using neural networks”, IEEE Transactions on Energy Conversion, vol. 14, no. 4, pp. 1572–1577, 1999.
[24] A. Al-moudi, L. Zhang, “Application of radial basis function networks for solar array modeling and maximum power point prediction”, IEE Proceedings, vol. 147, no. 5, pp. 310–316, 2000.
[25] A. Hussein, K. Hirasawa, J. Hu, J. Murata, “The dynamic performance of photovoltaic supplied dc motor fed from DC–DC converter and controlled by neural networks”, In Proc. Int. Joint Conf. Neural Netw, pp. 607–612, 2002.
[26] X. Sun, W. Wu, X. Li, Q. Zhao, “A research on photovoltaic energy controlling system with maximum power point tracking”, In Proc. Power Convers. Conf., pp. 822–826, 2002.
[27] R.M. Hilloowala, A.M. Sharaf, “A rule-based fuzzy logic controller for a PWM inverter in photo-voltaic energy conversion scheme”, In Proc. IEEE Ind. Appl. Soc. Annu. Meet., pp. 762–769, 1992.
[28] C.Y. Won, D.H. Kim, S.C. Kim, W.S. Kim, H.S. Kim, “A new maximum power point tracker of photovoltaic arrays using fuzzy controller”, In Proc. 25th Annu. IEEE Power Electron. Spec. Conf., pp. 1033-1038, 1994.
[29] T. Senjyu, K. Uezato, “Maximum power point tracker using fuzzy control for photovoltaic arrays”, In Proc. IEEE Int. Conf. Ind. Technol., pp. 143–147, 1994.
[30] G.J. Yu, M.W. Jung, J. Song, I.S. Cha, I.H. Hwang, “Maximum power point tracking with temperature compensation of photovoltaic for air conditioning system with fuzzy controller”, In Proc. IEEE Photovoltaic Spec. Conf., pp. 1429–1432, 1996.
[31] M.G. Simoes, N.N. Franceschetti, M. Friedhofer, “A fuzzy logic based photovoltaic peak power tracking control”, In Proc. IEEE Int. Symp. Ind. Electron., pp. 300–305, 1998.
[32] C.B. Salah, M. Ouali, “Comparison of fuzzy logic and neural network in maximum power point tracker for PV systems”, Electric Power Systems Research, vol. 81, pp. 43–50, 2011.
[33] M.M. Algazar, H. AL-monier, H.A. EL-halim, M.E. El Kotb Salem, “Maximum power point tracking using fuzzy logic control”, Electrical Power and Energy Systems, vol. 39, pp. 21–28, 2012.
[34] S. Danyali, M. Babaeifard, M. Shirkhani, A. Azizi, J. Tavoosi, Z. Dadvand, "A new neuro-fuzzy controller based maximum power point tracking for a partially shaded grid-connected photovoltaic system", Heliyon, vol. 10, no. e36747, pp. 1-17, 2024.
[35] Z. Boumous, S. Boumous, "Novel Intelligent control of photovoltaic system using ANFIS Gravitational Search for MPPT controller", Przegląd Elektrotechniczny, vol. 100, no. 7, pp. 1-5, 2024.
[36] K. Eetivand, A. Zangeneh, S.M.H. Nabavi, "Hyper-Spherical Search Algorithm for Maximum Power Point Tracking of Solar Photovoltaic Systems under Partial Shading Conditions", International Transactions on Electrical Energy Systems, vol. 2022, pp. 1-18, 2022.
[37] A.R. Reisi, M.H. Moradi, S. Jamasb, "Classification and comparison of maximum power point tracking techniques for photovoltaic system: A review", Renewable and Sustainable Energy Reviews, vol. 19, pp. 433-443, 2013.
[38] P. Hu, A. Ukil, N.C. Nair, "Maximum Power Point Tracking Algorithm Based on Adaptive Particle Swarm Optimization Under Partial Shading Conditions", in 2023 49th Annual Conference of the IEEE Industrial Electronics Society (IECON), October 2023.
[39] K. Aygül, M. Cikan, T. Demirdelen, M. Tumay, "Butterfly optimization algorithm based maximum power point tracking of photovoltaic systems under partial shading condition", Energy Sources, Part A: Recovery, Utilization, and Environmental Effects, pp. 1-18, 2019.

[40] M.H.M. Jahromi, H.D. Tafti, S.M. Hosseini, A. Jalali, M. Keivanimehr, "Maximum Power Point Tracking of a Network-Connected Photovoltaic System Based on Gravity Search Algorithm and Fuzzy Logic Controller", Journal of Solar Energy Research Updates, vol. 7, pp. 52-63, 2020.
[41] I. Pervez, A. Pervez, M. Tariq, A. Sarwar, M. Zaid, A. Riyaz, "A Maximum Power Point Tracking Method for a Partially Shaded Solar PV Cell using PSO with Damped Inertial Weight Algorithm and Time varying Acceleration", in 2019 1st International Conference on Energy, Power and Environment: Towards Clean Energy Technologies, June 2019.
[42] A. Sharma, D.K. Palwalia, "Synergistic Application of Particle Swarm Optimization and Gravitational Search Algorithm for Solar PV Performance Improvement", Advances in Information Technology, vol. 5, no. 2, pp. 1-11, 2024.
[43] H. Khaterchi, C.B. Regaya, A. Jeridi, A. Zaafouri, "Innovative Hybrid War Strategy Optimization with Incremental Conductance for Maximum Power Point Tracking in Partially Shaded Photovoltaic Systems", Power Electronics and Drives, vol. 10, no. 45, pp. 1-18, 2025.
[44] D. Mazumdar, C. Sain, P.K. Biswas, P. Sanjeevikumar, B. Khan, "Overview of Solar Photovoltaic MPPT Methods: A State of the Art on Conventional and Artificial Intelligence Control Techniques", International Transactions on Electrical Energy Systems, vol. 2024, pp. 1-24, 2024.
[45] I. Sajid, A. Gautam, A. Sarwar, M. Tariq, H.D. Liu, S. Ahmad, C.H. Lin, A.E. Sayed, "Optimizing Photovoltaic Power Production in Partial Shading Conditions Using Dandelion Optimizer (DO)-Based MPPT Method", Processes, vol. 11, no. 8, pp. 1-28, 2023.
[۴۶] سید محمد مهدی حاج ابوترابی و محمد سروی، «یک روش جدید برای تعیین و ردیابی نقطه حداکثر توان آرایه خورشیدی»، مجله مهندسی برق دانشگاه تبریز، جلد۴۹، شماره۴، صفحات ۱۵۶۰-۱۵۶۷- ۱۳۹۸.
[۴۷] سید مجید هاشم زاده و محمد هجری، «یک روش جدید برای ردیابی نقطه حداکثر توان سرتاسری در آرایه های خورشیدی شامل چند ردیف موازی تحت شرایط سایه جزئی»، مجله مهندسی برق دانشگاه تبریز، جلد۴۹، شماره۴، صفحات ۱۸۸۴-۱۸۹۴-۱۳۹۸.